Original Article

Quality assurance of CT number–relative electron density conversion table for dose calculation using CT images with single energy projection-based MAR technique

Shogo Hatanaka [1)], Kazutoshi Kodama [1)], Tetsuya Watanabe [1)], Masatsugu Hariu [1)], Rikana Soda [1)], Kana Washizu [1)], Nobuko Utsumi [1,2)], Takafumi Yamano [1)], Keiichiro Nishimura [1)], Keisuke Todoroki [1)], Katsuhito Hosaka [1)], Munefumi Shimbo [1)], Takeo Takahashi [1)]

[1)] Department of Radiation Oncology, Saitama Medical Center, Saitama Medical University
[2)] Department of Radiology, JCHO Tokyo Shinjuku Medical Center

Abstract

A metal artifact reduction (MAR) technique can reduce beam hardening and streak artifacts caused by metal in the body on computed tomography (CT). In this study, we evaluated a CT number–relative electron density (CT-rED) conversion table in dose calculation using CT images with MAR technique. **Materials and methods:** CT images of a RMI-467 cylinder-type solid water phantom, 16 normal rods (rED: 0.28 to 1.69), a titanium rod (3.79) and a stainless-steel rod (6.58) were acquired for the CT-rED table. Four CT-rED tables were created using the CT images with single energy projection-based MAR techniques: $normal_{raw}$ (without MAR), normal, normal + titanium and normal + titanium + stainless steel. The CT numbers were compared between CT-rED tables $normal_{raw}$ and normal. CT images of 23 patients (36 plans and 159 beams in total) were used. Monitor unit (MU) calculations were performed using each CT-rED table and each patient's data. The differences of the MUs acquired using the high-density material data relative to those of the MUs acquired using normal CT-rED table were calculated. **Results:** The changes in CT number due to MAR were very small (0.1 ± 3.2 HU). The greater the maximum rED input to the CT-rED table, the greater the variation of the calculated dose. Nevertheless, all relative differences were within 1%. **Conclusion:** The creation of a dedicated CT-rED conversion table for the CT images with single energy projection-based MAR techniques might not be necessary.

key words Radiation therapy, computed tomography, CT number–relative electron density conversion table, metal artifact reduction technique

Corresponding author: Shogo Hatanaka
Department of Radiation Oncology, Saitama Medical Center, Saitama Medical University
1981, Kamoda, Kawagoe City, Saitama 350-8550, Japan
Phone: +81-049-2283511 Fax: +81-049-2283753
Received December 10th, 2018 / Accepted after revision February 3rd, 2019

Introduction

Most radiation treatment plans are based on computed tomography (CT) images. However, if a metal implant is located near a tumor, it becomes difficult to define target volume and to calculate dose distribution accurately. Influence of metal artifacts can be reduced, and accuracy of target volume calculation can be improved by metal artifact reduction (MAR) techniques [1-5]. Therefore, CT images based on MAR techniques are useful for planning radiation treatment regimens and extensive use of CT images is expected in the future.

In conventional methods, if metal implants are contained in CT slices, restriction of beam angles is required to exclude the metal implants from radiation fields. Additionally, since accurate calculation of dose distribution is difficult because of presence of metal artifacts, most dose calculation is performed without heterogeneous correction. With CT-image-based dose calculation using MAR techniques, more accurate dose distributions can be achieved without restricting beam angles.

In most commercial algorithms for CT-image-based dose calculation, CT numbers are converted to relative electron density (rED) of water using a computed tomography–relative electron density (CT-rED) conversion table installed in a radiation treatment planning system (RTPS). The effect of MAR techniques on CT numbers has been hardly verified, thus it remains unclear whether creation of a dedicated CT-rED conversion table for CT images based on MAR techniques is required. Additionally, CT numbers which are equivalent to values of human tissues are commonly inputted into CT-rED tables for clinical use. CT numbers of high-density materials, such as metal implants, are much greater than those of human tissues. Therefore, it is required for accurate dose calculation with CT images including high-

Table 1.
Electron density relative to water and the physical density of the rods used in this study.

Rod material	Electron density relative to water	Physical density (g/cm^3)
Lung (LN-300)	0.28	0.30
Lung (LN-450)	0.40	0.45
Adipose (AP6)	0.90	0.92
Breast	0.96	0.99
Solid water*	0.99	1.02
Brain	1.05	1.05
Liver (LV1)	1.07	1.08
Inner bone	1.09	1.12
Bone (B200)	1.11	1.15
Bone (CB2-30% mineral)	1.28	1.34
Bone (CB2-50% mineral)	1.47	1.56
Cortical bone (SB3)	1.69	1.82
True water	1.00	1.00

*Four solid water rods were used.

density materials to add very high CT numbers and rEDs to CT-rED tables. In RTPS, gradation numbers of rED are defined. Thus, the greater maximum rED inputted into a CT-rED table become, the greater rED per gradation become. Several reports have evaluated dose distributions around metal implants [6-8]; however, the effect of adding high-density material data to a CT-rED table on the calculated dose has not yet been investigated. For quality assurance of the CT-rED table in dose calculation using CT images with single energy projection-based MAR techniques, we evaluated the effect of MAR techniques on CT numbers and the variations in calculated dose upon addition of high-density material data to the CT-rED table.

Materials and methods

Ethical approval

This study protocol was approved by the Ethics Committees of Saitama Medical Center.

Acquisition of CT-rED tables

An Optima CT system (GE Healthcare, Piscataway, NJ, USA) was used for acquisition of CT images. A cylinder-type solid water phantom (RMI-467; GAMMEX RMI GmbH, Biebertal, Germany) was used for acquiring of the CT-rED tables. Sixteen rods were inserted into this phantom and then CT images of the phantom and the rods were acquired. The appearance of the phantom and the rods is shown in **Fig. 1a**. The rods were made of materials whose electron densities were from 0.28 to 1.69 relative to electron density of water (**Table 1**). Acquiring conditions of CT images were the same as those during clinical use (tube voltage: 120 kVp). CT numbers of each rod were acquired and two CT-rED tables were created: one using CT images without MAR techniques (CT-rED table A_{raw}) and the other with MAR techniques (CT-rED table A). Additionally, an rED of 0.01, which was equivalent to a CT number of − 990, was inputted into the CT-rED table as a minimum rED (and a minimum CT number). Mean difference between CT numbers with and without MAR techniques was calculated (with MAR–without MAR).

Then, one rod was replaced with a titanium rod (rED 3.79; 1.5 cm ϕ; GAMMEX RMI GmbH) and its CT images were acquired and

(a) | (b)

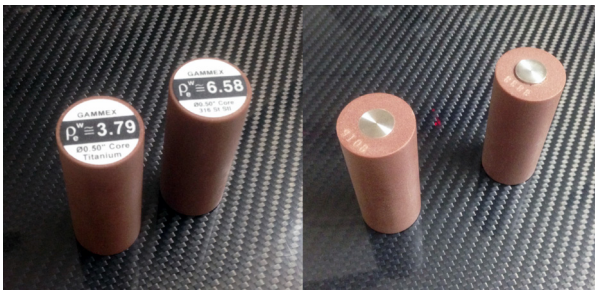

Figure 1:
(a) Phantom and rods used in the study. Sixteen rods were inserted into this phantom and CT images of the phantom and rods were acquired. The rods were made of materials with electron densities of 0.28 to 1.69 relative to water.
(b) Titanium (left panel) and stainless-steel (right panel) rods used in the study. A relative electron density of titanium rod is 3.79, and that of a stainless-steel rod is 6.58.

reconstructed using MAR techniques. A CT number of the titanium rod was got and data about the CT number and rED of the titanium rod were added to CT-rED table A (CT-rED table A + titanium data = CT-rED table B). Similarly, a CT number of a stainless-steel rod (rED 6.58; 1.5 cm ϕ; GAMMEX RMI GmbH) was acquired and data about the CT number and rED of stainless steel were added to CT-rED table B (CT-rED table B + stainless-steel data = CT-rED table C). Regarding acquisition of each CT number, three times of measurements were performed, respectively. **Figure 1b** shows appearance of the titanium rod and the stainless-steel rod.

Dose calculation using CT images

XiO version 5.00 RTPS (Elekta AB, Stockholm, Sweden) was used in this study to acquire CT images of 23 patients (a total of 36 plans and 159 beams) treated at our institution. Of these, 31 plans and 119 beams (head and neck, thorax, abdomen, breast and spine, including field-in-field techniques) of 18 patients were obtained for conventional three-dimensional conformal radiation therapy (3D-CRT), and five plans and 40 beams of five patients were obtained for lung stereotactic body radiation therapy (SBRT). Because the purpose of this study was only to evaluate effect of adding high-density material data to a CT-rED table on the calculated dose, cases into whom metal implants were inserted were not included in this study. Slice thicknesses of CT images used for conventional 3D-CRT plans were 2.5 mm and those used for lung SBRT plans were 1.25 mm.

Dose distribution and monitor unit (MU) calculations were performed with data of each patient by using CT-rED table A. Calculations

Table 2. The effect of MAR techniques on CT numbers.

Rod material	CT number without MAR Mean ± 1 SD (HU)	CT number with MAR Mean ± 1 SD (HU)	Mean difference between CT number with MAR and without MAR
Lung (LN-300)	− 692.9 ± 16.8	− 694.8 ± 20.1	− 1.9
Lung (LN-450)	− 534.0 ± 13.9	− 541.0 ± 22.1	− 7.0
Adipose (AP6)	− 84.1 ± 17.9	− 85.6 ± 18.3	− 1.5
Breast	− 29.4 ± 17.9	− 27.7 ± 17.7	1.7
Solid water	11.9 ± 15.9	13.6 ± 16.8	1.7
Brain	35.5 ± 19.2	34.0 ± 18.5	− 1.5
Liver (LV1)	91.0 ± 19.2	96.6 ± 18.7	5.6
Inner bone	236.6 ± 15.3	236.1 ± 16.4	− 0.5
Bone (B200)	242.2 ± 18.5	240.4 ± 19.6	− 1.8
Bone (CB2-30% mineral)	455.1 ± 22.0	457.9 ± 24.2	2.8
Bone (CB2-50% mineral)	816. 9 ± 20.3	821.0 ± 24.0	4.1
Cortical bone (SB3)	1207.4 ± 24.0	1207.4 ± 25.6	-0.0
True water	6.7 ± 18.2	6.1 ± 20.4	-0.6

HU, Hounsfield unit

were also performed by using CT-rED table B and C. Algorithm of superposition [9,10] with heterogeneous correction was used for dose calculation. A linear accelerator (linac) models Varian linac Clinac-21EX (6, 10 MV X-ray) and Varian linac Clinac-21EX (4, 10 MV X-ray) were used in this study. Differences in MUs acquired using high-density material data relative to those acquired using CT-rED table A were calculated. In addition, effects of differences between dose calculation grid sizes (2, 3, and 5 mm) were verified.

Statistical analysis

With regard to relative differences in MUs calculated using each CT-rED table, a paired *t*-test was used to assess mean differences among CT-rED table B group and CT-rED table C group. And, with regard to MUs calculated using each CT-rED table containing high-density material data relative to those in MUs calculated using CT-rED table A, Pearson correlation coefficients (r) with p-values were calculated. In addition, An ANOVA (Analysis of Variance) test was performed to assess statistical significance between the dose calculation grid sizes. Differences were considered significant if two-tailed *p*-value was <0.01. SPSS for Windows version 23 software (IBM, Armonk, NY, USA) was used for statistical analysis.

Results

As shown in **Table 2**, the effect of MAR techniques on CT number was very small. **Figure 2** shows the CT-rED tables acquired in this study (**figure 2a**) and the CT images of phantom (**figure 2b**). The maximum CT numbers inputted into CT-rED tables A, B and C were 1207, 7520 and 12234, respectively.

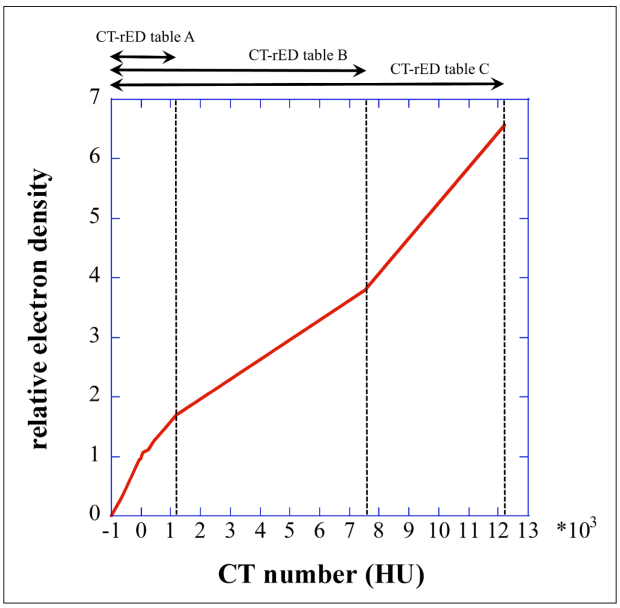

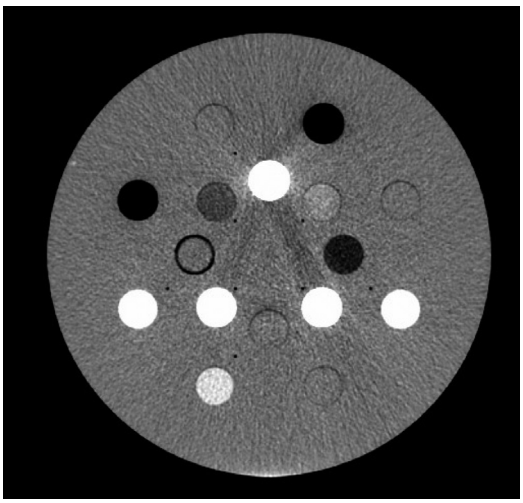

(a) | (b)

Figure 2:

(a) Computed tomography–relative electron density (CT-rED) tables obtained in the study. The maximum CT numbers input to CT-rED tables A, B and C were 1207, 7520 and 12234, respectively.

(b) The CT images of phantom for acquisition of the CT-rED table.

Table 3 shows the comparison of MUs between tables A, B and C. The mean differences of MUs between each CT-rED table were very small.

Figure 3 shows Bland-Altman analysis for 3D-CRT (a: CT- rED table A vs B, b: CT- rED table A vs C). The mean differences ± standard deviation (SD) were -0.03 ± 0.05 and -0.06 ± 0.09, respectively. The larger the maximum CT number and rED inputted into the CT-rED table became, the greater the relative differences became (paired *t*-test: $p < 0.01$).

Figure 4 shows Bland-Altman analysis for lung SBRT (a: CT- rED table A vs B, b: CT-rED table A vs C). The mean differences ± SD were -0.05 ± 0.17 and -0.16 ± 0.32, respectively. The larger the maximum CT number and rED inputted into the CT-rED table became, the greater the relative differences became (paired *t*-test: $p < 0.01$). And, the maximum difference of lung SBRT was slightly larger than that of 3D-CRT.

Figure 5 shows the comparison among the results for grid sizes of 2, 3 and 5 mm (a: CT-rED table A vs B, b: CT- rED table A vs C) and

Table 3. The comparison of monitor units (MU) between table A, B and C.

	MU (mean ± SD)		
Grid size	2 mm	3 mm	5 mm
table A	89.20 ± 56.29	89.36 ± 56.40	89.73 ± 56.74
table B	89.17 ± 56.27	89.32 ± 56.37	89.69 ± 56.71
table C	89.12 ± 56.24	89.27 ± 56.33	89.64 ± 56.68

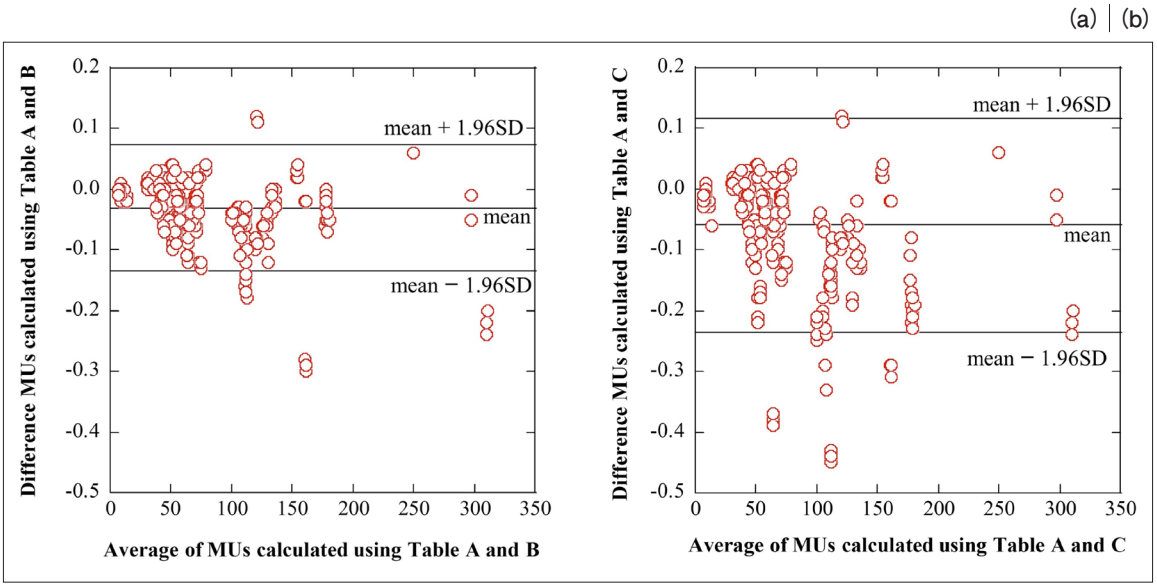

Figure 3:
Bland-Altman analysis for 3D-CRT (a: CT- rED table A vs B, b: CT- rED table A vs C). The mean differences ± standard deviation (SD) were -0.03 ± 0.05 and -0.06 ± 0.09, respectively. The larger the maximum CT number and rED inputted into the CT-rED table became, the greater the relative differences became (paired *t*-test: $p < 0.01$).

Pearson correlation coefficients (r) with p-values. No definite trend as a function of grid size was found (ANOVA test: $p = 0.962$).

The mean and SD of relative differences for all results were −0.1 ± 0.1%, and all relative differences were within 1.0%.

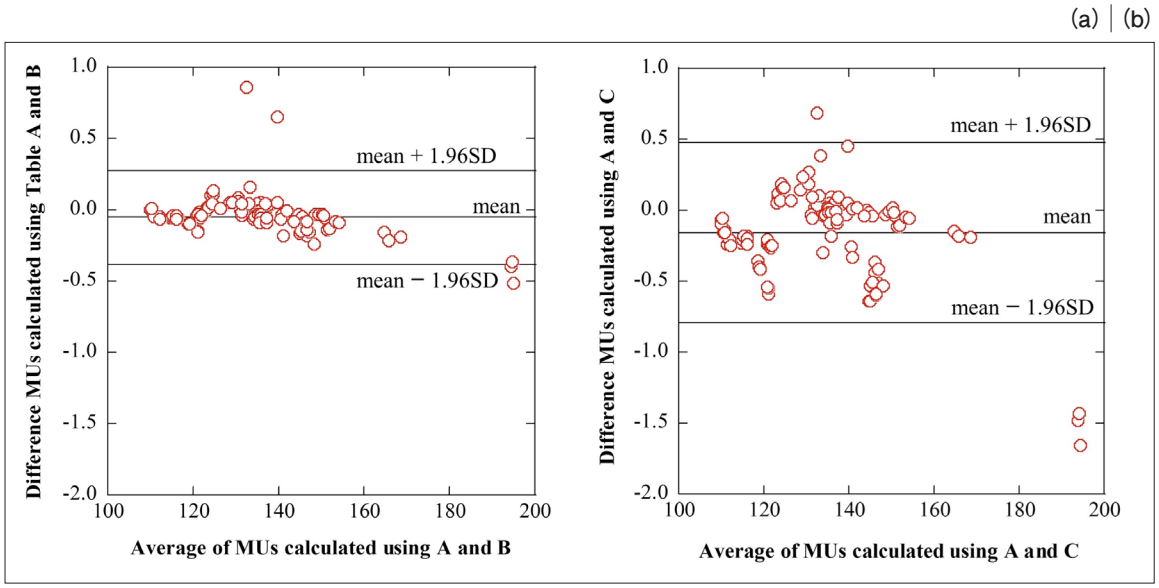

Figure 4:
Bland-Altman analysis for lung SBRT (a: CT- rED table A vs B, b: CT- rED table A vs C). The mean differences ± SD were -0.05 ± 0.17 and -0.16 ± 0.32, respectively. The larger the maximum CT number and rED inputted into the CT-rED table became, the greater the relative differences became (paired t-test: $p < 0.01$). And, the maximum difference of lung SBRT was slightly larger than that of 3D-CRT.

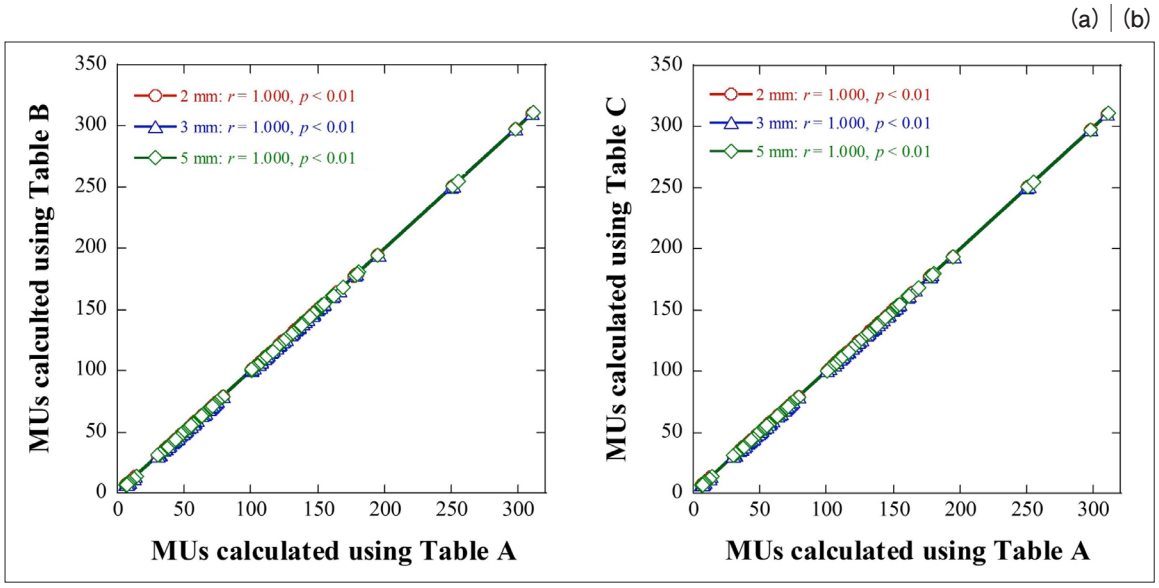

Figure 5:
Comparison among the results for grid sizes of 2, 3 and 5 mm (a: CT- rED table A vs B, b: CT- rED table A vs C) and Pearson correlation coefficients (r) with p-values. No definite trend as a function of grid size was found (ANOVA test: p =0.962).

Discussion

As a result, it was clarified that the effect of MAR techniques on CT numbers was very small. And, the greater the maximum CT number inputted into the CT-rED table became, the greater the variation of the calculated dose became. In the dose calculation using the XiO, the CT numbers were converted to rED and then discretized to the defined gradation. The greater the difference between the minimum rED and the maximum inputted into the CT-rED table became, the greater the rED per gradation became, which was a cause of the variation of the calculated dose. In addition, the maximum differences of lung SBRT were larger than those of conventional 3D-CRT. In the case of strong heterogeneous regions, the effect of the differences of CT-rED tables might be larger. Nevertheless, all relative differences were within 1%. Therefore, the effect of adding high-density material data to the CT-rED table on calculated dose was very small.

No definite trend as a function of grid size was found. Grid sizes of 2 to 5 mm are generally used in clinical practice. Therefore, in relation to the effect of adding high-density material data to the CT-rED table on the calculated dose, the difference in grid size might be negligible.

The effects of MAR techniques on CT numbers and of adding high-density material data to the CT-rED table on the calculated dose were very small. Thus, it might not be necessary to create a dedicated CT-rED conversion table for the CT images with single energy projection-based MAR techniques.

As limitations to this study, the effect on dose distribution was not verified. However, because the change of MUs was very small, it was expected that the effect on dose distribution was also small. And, materials whose density were higher (CT number) than stainless steel were not used in this study, so we don't recommend adding higher CT numbers to CT-rED tables. In addition, the monochromatic images based on dual energy CT, which is another MAR technique, was not considered in this study, thus further investigations are warranted to explore this topic.

Conclusions

CT images based on MAR techniques are useful for planning radiation treatment and, therefore, may be used extensively in the future. However, relatively few reports have focused on accuracy of dose calculations using CT images with single energy projection-based MAR techniques. In this study, the effects of MAR techniques on CT numbers and of adding high-density material data to the CT-rED table on the calculated dose were very small. Therefore, the creation of the dedicated CT-rED conversion table for CT images with single energy projection-based MAR techniques might not be necessary.

References

1. Giantsoudi D, De Man B, Verburg J, et al. Metal artifacts in computed tomography for radiation therapy planning: dosimetric effects and impact of metal artifact reduction. Phys Med Biol. 2017 21;62 (8) :R49-R80.
2. Teixeira PA, Meyer JB, Baumann C, et al. Total hip prosthesis CT with single-energy projection-based metallic artifact reduction: impact on the visualization of specific periprosthetic soft tissue structures. Skeletal Radiol 2014;43:1237–46.
3. Jeong S, Kim SH, Hwang EJ, et al. Usefulness of a metal artifact reduction algorithm for orthopedic implants in abdominal CT: phantom and clinical study results. AJR Am J Roentgenol 2015; 204: 307–17.
4. Wang Y, Qian B, Li B, et al. Metal artifacts reduction using monochromatic images from spectral CT: evaluation of pedicle screws in patients with scoliosis. Eur J Radiol 2013;82: e360–6.
5. Yu L, Leng S, McCollough CH. Dual-energy CT-based monochromatic imaging. AJR Am J Roentgenol 2012;199: S9–15.
6. Chin DW, Treister N, Friedland B, et al. Effect of dental restorations and prostheses on radiotherapy dose distribution: a Monte Carlo study. J Appl Clin Med Phys 2009;10:2853.
7. Farahani M, Eichmiller FC, McLaughlin WL. Measurement of absorbed doses near metal and dental material interfaces irradiated by x- and gamma-ray therapy beams. Phys Med Biol 1990;35:369–85.
8. Nadrowitz R, Feyerabend T. Backscatter dose from metallic materials due to obliquely incident high-energy photon beams. Med Phys 2001;28:959–65.
9. Miften M, Wiesmeyer M, Monthofer S, et al. Implementation of FFT convolution and multigrid superposition models in the FOCUS RTP system. Phys Med Biol 2000;45:817–33.
10. Miften M, Wiesmeyer M, Kapur A, et al. Comparison of RTP dose distributions in heterogeneous phantoms with the BEAM Monte Carlo simulation system. J Appl Clin Med Phys 2001;2:21–31.